

Proposed Methods to Increase the Output Efficiency of a Photovoltaic (PV) System

Fatima Zohra Zerhouni, M'hamed Houari Zerhouni, Mansour Zegrar, M. Tarik Benmessaoud, Amine Boudghene Stambouli, Abdelhamid Midoun

Electronics Department

University of Sciences and Technology Mohamed Boudiaf (U.S.T.M.B.O)

BP 1505, Oran El M'Naouer, Oran, Algérie

E-mail: zerhouni_fz@yahoo.fr, aboudghenes@yahoo.com

Abstract: Lately, the use of solar energy has seen considerable development. Transformation in electric energy is one of its applications which attracts considerable interest, owing to the fact that it makes it possible to solve a major problem in isolated cities that lack electrical supply networks. For solar energy use, the current drawback remains its high cost. This problem can be resolved through different improvements in terms of power production. For that, different axis of research can be explored [1-3].

Over the past few years, solar cells arrays (SCA) have been connected to various loads in a direct coupled method. A PV module can produce the power at a point, called an operating point, anywhere on the current- voltage (I-V) curve. The coordinates of the Operating point are the operating voltage and current. There is a unique point near the knee of the I-V curve, called a maximum power point (MPP), at which the module operates with the maximum efficiency and produces the maximum output power. The point of maximum power is the desired operating point for a PV array to obtain maximum efficiency. A PV array is usually oversized to compensate for a low power yield during winter months. This mismatching between a PV module and a load requires further over-sizing of the PV array and thus increases the overall system cost [3-5]. To mitigate this problem, different methods have been developed [6-12]. A maximum power point tracker (MPPT) can be used to maintain the PV module's operating point at the MPP. The system in a direct coupled method cannot always operate at maximum power point (MPP) of the solar array when the load, irradiance or temperature changes. A PV-load coupling system should be able to maximize the energy output of the PV generator, which should operate always at its maximum power point (MPP) in order to achieve maximum global efficiency. Some authors have supported the direct coupling between the PV generator and the load [2-3]. Several methods and algorithms to track the maximum power point have been developed [2-12].

We focused our effort on improving the matching between PV sources and loads through the development of new performing methods. In this paper, a rapid approach for peak power tracking is proposed. The system PV generator - load is optimized, when the working point in direct coupling is quite near the MPP of the PV generator, so that the global efficiency of the system is acceptable. Another method is proposed. It is based on reconfiguring on-line the SCA by changing the connections between different modules in

order to minimize the losses due to load and operation conditions. Two strategies for improvements are chosen for testing in this study, whatever the loads and operating conditions.

The experimental system used a microcontroller. It is robust when undergoing environment changes and load variations. The performance of the methods is verified through simulations and experiments.

Keywords: photovoltaic; MPPT; configuration; optimum power; switching

1 Introduction

The conversion of solar energy into electric energy is performed by means of photovoltaic (PV) generators. Photovoltaic offer the highest versatility among renewable energy technologies. Electricity produced from photovoltaic (PV) systems has a far smaller impact on the environment than traditional methods of electrical generation. The most attractive features of solar panels are the nonexistence of movable parts, the very slow degradation of the sealed solar cells and the extreme simplicity of its use and maintenance. Another advantage is the modularity. All desired generator sizes can be realized, from the mill watt range to the megawatt range. Solar energy is a pollution-free source of abundant power. During their operation, PV cells need no fuel, give off no atmospheric or water pollutants and require no cooling water. The use of PV systems is not constrained by material or land shortages and the sun is a virtually endless energy source.

2 Modeling of A PV Generator

The basic component of a SCA (solar cells array) is the photovoltaic cell. A photovoltaic (PV) array under uniform irradiance E_s exhibits a current-voltage characteristic with a unique maximum power point (MPP) where the array produces maximum output power, which changes as a consequence of the variation of the irradiance level and of the SCA temperature T [3-12].

The simple equivalent circuit is sufficient for most applications. Likewise, the PV generator current and, consequently, the power vary with the cells' operation temperature T and irradiance E_s . A photovoltaic array can be represented by an equivalent circuit composed of a current generator, a sensitive diode D to the light, a series resistor R_s and a shunt resistance R_{sh} , as shown in Figure 1.

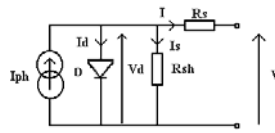


Figure 1

Equivalent circuit of a PV cell

By inspection of Figure 1, Kirchhoff's first law provides the current–voltage(I-V) characteristics. One can write the equation [3]:

$$I = I_{ph} - I_d - I_s \quad (1)$$

$$I_d = I_o \cdot \left[\exp\left(\frac{V_d}{A.U_T}\right) - 1 \right] \quad (2)$$

Where

I_{ph} is the photocurrent source equal to the short-circuit current I_{cc}

I_d is the generated current,

I_o is the saturation current of a solar array,

q is the electron charge,

K_B is the Boltzmann's constant,

and A is the ideality factor for a p–n junction.

$$I = I_{ph} - I_o \cdot \left[\exp\left(\frac{V_d}{A.U_T}\right) - 1 \right] - \frac{V_d}{R_{sh}} \quad (3)$$

$$\text{Or } V_d = V + R_s \cdot I \quad (4)$$

then,

$$I = I_{ph} - I_o \cdot \left[\exp\left(\frac{V + R_s \cdot I}{A.U_T}\right) - 1 \right] - \frac{V + R_s \cdot I}{R_{sh}} \quad (5)$$

By considering R_{sh} very large, one can approximate (5) by:

$$I = I_{cc} - I_o \cdot \left[\exp\left(\frac{V + R_s \cdot I}{A.U_T}\right) - 1 \right] \quad (6)$$

$$V = -R_s \cdot I + A U_T \cdot \ln \left[\frac{I_{cc} - I + I_o}{I_o} \right] \quad (7)$$

The equation (6) of the cell current I depends on the cell voltage V with the saturation current I_o and the diode factor A .

The expression (6) can represent the operation of a solar cell appropriately, but it presents some inconveniences in practical use. The expression possesses an implicit character: the current appears on both sides of the equation, forcing its solution through iterative methods or approximate solutions. The Newton Raphston iterative method is used.

Photovoltaic systems are designed around the photovoltaic cell. Since a typical photovoltaic cell produces less than 3 watts at approximately 0.5 volt dc, cells must be connected in series or/and in parallel configurations to produce enough power for high-power applications. In our case, a photovoltaic module is constituted of 36 solar polycrystalline cells in series (Kyocera LA 361 K51) mounted 35° south. Figure 2 illustrates the operating characteristic curves of the solar array under given irradiance and temperature. In Figure 2, V and I are the output voltage and the output current of the SCA, respectively. P is the power. A photovoltaic array under uniform irradiance E_s and fixed temperature T exhibits a current-voltage characteristic with a unique point, called the maximum power point (MPP), where the array produces maximum output power P_{opt} (Figure 2).



Figure 2

Electrical characteristic of the SCA at $E_s=100\%$, $T=25^\circ\text{C}$

$$P = V \cdot I = -R_s \cdot I^2 + A U_T \cdot I \cdot \ln \left[\frac{I_{cc} - I + I_o}{I_o} \right] \quad (8)$$

The curve in Figure 2a consists of different regions: one is the current source region, and the other is the voltage source region. In the voltage source region, the internal impedance of the solar array is low on the right side of the power curve, and in the current source region, the internal impedance of the solar array is high on the left side of the power curve. The maximum power point of the solar array is located at the knee of the power curve (zone 3). According to the maximum power transfer theory, the power delivered to the load is maximum when the source internal impedance matches the load impedance in a direct coupling. The peak P_{opt} in Figure 2 is provided by solving the following equation [3]:

$$\frac{dP}{dI} = -2.R_s.I + A.U_T.Ln\left[\frac{I_{cc} - I + I_o}{I_o}\right] - \frac{A.U_T.I}{I_{cc} - I + I_o} = 0 \tag{9}$$

The current I_{opt} is the solution of the following equation:

$$I_{cc} = I_{opt} + I_o \cdot \left[\exp\left[\frac{(2.I_{opt}.R_s)}{A.U_T} + \frac{I_{opt}}{I_{cc} - I_{opt} + I_o}\right] - 1 \right] \tag{10}$$

I_{opt} is replaced in equation (7) to obtain V_{opt} . The product $V_{opt} \cdot I_{opt}$ result in the optimal power P_{opt} . There is a unique P_{opt} on each P–V characteristic curve. V_{opt} and I_{opt} varie according to the sun irradiation ant temperature. Figure 3 shows the characteristic curves at different irradiances E_s . Figure 4 shows the characteristic curves at different temperatures T .

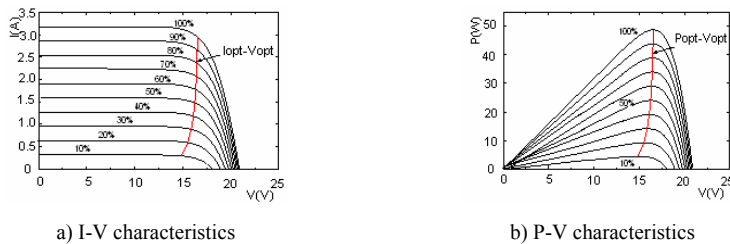


Figure 3

I-V and P-V characteristics of a solar module under varied solar irradiance

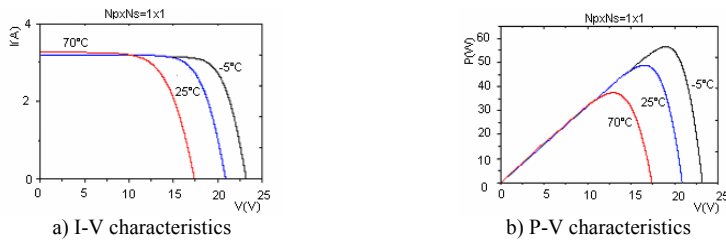


Figure 4

I-V and P-V characteristics of a solar module under varied temperatures

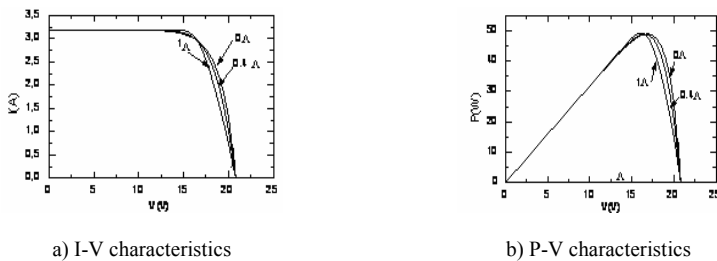


Figure 5

Influence of the series resistance R_s on the I-V and P-V characteristics of a PV module

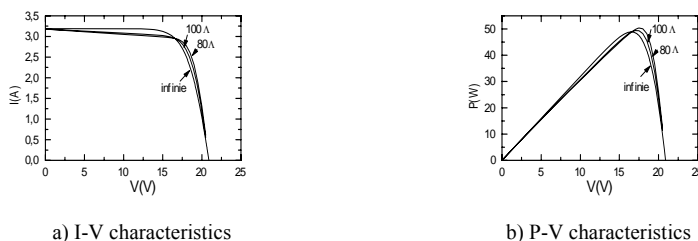


Figure 6

Influence of the series resistance R_{sh} on the characteristics of a PV module

The series resistance and the shunt resistance of the panel have a large impact on the slope of the I-V curve, as seen in Figures 5 and 6 respectively.

3 The Maximum Power Point Tracker

3.1 Introduction

Maximum Power Point Tracker (MPPT) is often used to increase the energy conversion efficiency for a photovoltaic energy source. The maximum power is transferred to the load when the impedance source matches the load one. To accomplish this objective, a switching converter is placed between the PV source and the load. With an MPPT control, it is possible to reach the output panel characteristics around the optimal power point. The output power of photovoltaic (PV) panels varies with atmospheric conditions (solar irradiance level and temperature) as well as their optimum voltage (V_{opt}) and current (I_{opt}). It is crucial to operate the PV energy conversion systems near the maximum power point (MPP) to increase the power yield of the PV system. This problem has attracted the interest of several authors [3-12]. Maximum power point tracking (MPPT) algorithms are usually implemented in the power electronic interface between the PV panel and a load. Maximum power point matching of a PV array with the load maximises the energy transfer by operating the load as closely as possible to the MPP line of the PV output, whatever the loads and working conditions. In our case, a Maximum power point tracker is a DC to DC convertor.

3.2 Optimum Power Point Detector

The current-voltage curve in a PV generator changes with the irradiance and the temperature conditions. This situation implies the need for a specific dynamic searching algorithm for the maximum and safe power point of the coupling PV-load. So, a system is inserted between the SCA and the load as shown in Figure 7.

This system is called MPPT (Maximum Power Point Tracker). In order to make the most of the available solar energy for any load and working conditions, the MPP can be tracked by using the MPPT [3-12]. In Figure 7, the input voltage and current are respectively (V_1 , I_1). The output voltage and current are respectively (V_2 , I_2).

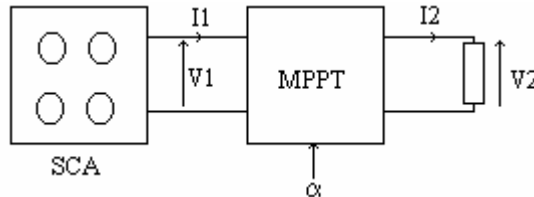


Figure 7

Connexion SCA – load via MPPT

α is the static converter duty cycle [3]. It is a control parameter. α varies. α allows an optimal impedance adaptation:

$$P_2 = P_1 \quad (11)$$

P_2 is the output power;

P_1 is the input power;

α_{opt} is determined by:

$$V_1 = V_{opt} \quad (12)$$

$$I_1 = I_{opt} \quad (13)$$

V_{opt} and I_{opt} are the optimal voltage and the optimal current respectively.

In general, α can be determined according to the load [3]. So the load parameters are required, but unfortunately these parameters are not constant. The study is then for a specific load and cannot be applicable if the load changes. Also, the optimal voltage V_{opt} and the optimal current I_{opt} depend on the climatic conditions, on the particular moment of the day and season. These variations are problems. Therefore, it is important to design a flexible system which can be adapted to large types of loads and under different operating conditions in order to reduce the mismatch losses in a directly coupled load to a SCA.

Another method is the fixed reference voltage control method. It is the simplest control method. This method regulates the solar array terminal voltage and matches it to a fixed reference voltage, which is the MPP of the SCA. Indeed, the V_{opt} variation according to V_{oc} (V_{oc} : the SCA open circuit voltage) is linear whatever the working conditions [3]. The approximation is:

$$V_{opt} = \frac{75 \cdot V_{oc}}{100} \quad (14)$$

α_{opt} is calculated according to:

$$\alpha_{opt} = \frac{V_2}{V_{opt}} \quad (15)$$

To measure V_{oc} , a pilot cell in open circuit is used. It is at the same SCA's working conditions.

$$V_{oc} = N_s \cdot V_{ocs} \quad (16)$$

V_{oc} : SCA open circuit voltage;

V_{ocs} : the cell pilot open circuit voltage;

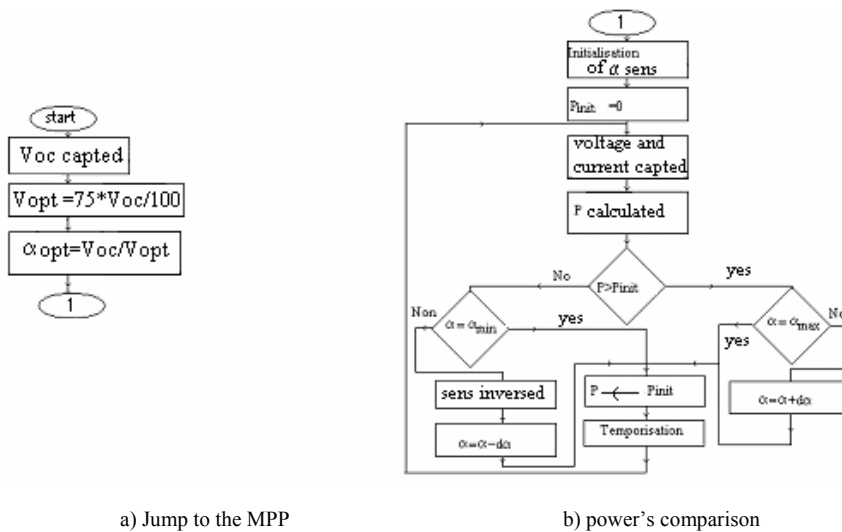
N_s : the series solar cell's number.

In practice, the V_{oc} value will be different from the real because the photovoltaic cells are not all identical. To overcome this problem, one measures real SCA V_{oc} while cutting off the load's supply for a short moment, without disturbing the system's operation. There is also another control method, independent of any knowledge of the SCA or the load characteristics, to find the optimum power point by comparing powers [3].

3.3 Adopted Method

We combined the methods practically. In the first time, in real time, the system is in open circuit. Model V_{opt} is calculated according to the equation (14). The voltage operation is measured. Then, the cyclic ratio is calculated, according to the relation (15). The principle is to adjust the actual operating point of the PV array so that the actual power P approaches the optimum value P_{opt} as closely as possible. This cyclic ratio brings the operation point around the optimum power point [3]. We then track the optimum power point tracking per powers comparison as shown in flowchart (Figure 8). According to the power's variation, the cyclic ratio is readjusted. At the end, the system will oscillate between three points which encircle the optimum power point.

Thus, in this zone, the optimum power point is then determined. The MPPT can always track the MPP. At this level, if the load and/or the irradiance change abruptly, the operating point is deviated from that optimal. The cyclic ratio is changed automatically, in a gradual way, until it reaches the MPP as shown in the flowchart in Figure 8b. However, to reduce the convergence time towards the optimum power point, a method is proposed. A relation between the new cyclic ratio to that preceding the change is established.



a) Jump to the MPP

b) power's comparison

Figure 8

MPP research flow chart

In Figure 9, one supposes that after having determined the MPP, the operating point is A'. A sudden increase in the load will bring back the operating point to the point B'. The cyclic ratio to adopt in this case is calculated according to:

$$\alpha'_{opt} = \frac{\alpha_{opt} \cdot V' \cdot I_{opt}}{V_{opt} \cdot I'} \quad (17)$$

with:

α_{opt} : Cyclic ratio around the MPP before the abrupt change;

I_{opt} : SCA current around the MPP before the change occurred;

V_{opt} : SCA voltage around the MPP before the abrupt change;

V' : SCA voltage after the abrupt change;

I' : SCA current after the abrupt change;

α'_{opt} : New cyclic ratio.

The point B' is brought back around the MPP at the point C (equation 17). Then, the MPP tracking by comparing powers is adopted (Figure 8b)).

Another case is studied. The operating point is A'. For an abrupt reduction in load, the new operating point is point A (Figure 9). The current in A and the current in A' are closed and closed to the SCA short circuit current. The cyclic ratio adopted to bring back the operating point A around the MPP (noted B) will be a particular case of the equation (14), according to:

$$\alpha'_{opt} = \frac{\alpha_{opt} \cdot V'}{V_{opt}} \tag{18}$$

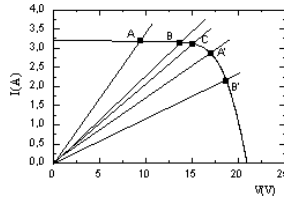


Figure 9
MPP research

3.4 Practical Results

The practical results consider a SCA of three modules in series. A DC buck converter has been realized experimentally and used. The experimental results are given below.

Figure 10 illustrates the practical results of the power P against the voltage V , for an irradiance $E_s=56\%$ and a temperature $T=27\text{ }^\circ\text{C}$. The MPP research characteristic in a gradual way is illustrated by Figure 10a. The operating point is initially at the point A ($V_A=20.06\text{ V}$, $I_A=1.76\text{ A}$, $P_A=35.41\text{ W}$). According to the algorithm established (Figure 8b) [3], the program compares the powers and readjusts gradually α to progress towards the MPP ($P_{opt}=76.92\text{ W}$, $V_{opt}=46.68\text{ V}$). The system operation will be stabilized at the end between the points 1, 2, and 3 which encircle the MPP.

Figure 10b illustrates the practical result for the same working conditions but by adopting the jump method towards the MPP according to the equations (17) and (18). Next, the method to move toward the MPP is by steps as shown in Figure 10b. It is seen that intermediate steps are avoided and convergence towards the MPP is fast. At the end, the system is operating between points 1, 2 and 3.

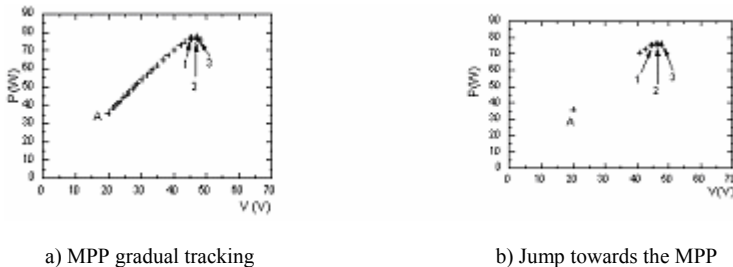


Figure 10

Experimental P-V characteristics, $E_s=56\%$, $T=27\text{ }^\circ\text{C}$

Another case is also verified practically. During the SCA operation, a sudden load change occurs. It generates the operating point's displacement towards a power lower than the optimum one. The operation point must thus be brought back towards the optimum power zone. The developed program calculates in real time the cyclic ratio to approach the MPP quickly. The result is shown in Figure 11. This Figure shows an example of the SCA current evolution.

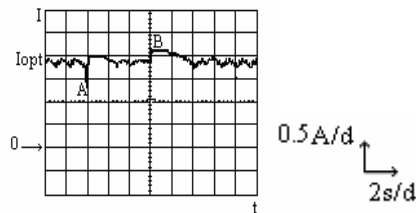


Figure 11

Experimental system response after abrupt load changes

The operating current is around I_{opt} , and an abrupt increase in the load (at "A") occurs. The current falls. The system calculates and adopts in real time α . So, an operation at I_{opt} occurred. Suddenly, at 'B', a load reduction occurs. The operating current increases. The system determines in real time α . The system's operation is stabilized gradually around the MPP at the I_{opt} current and an optimum operation is ensured. Our new MPPT control adjusts continually the static converter duty cycle. Transitory effects are immediately detected and the new MPP rapidly recovered. This method has been applied for a resistive load and for a DC motor. The MPP research has been successfully verified. The MPP is then rapidly recovered.

4 The Reconfiguration Method

4.1 Introduction

Another method presented in this paper is based on reconfiguring On-line the SCA by changing the connections between different modules in order to minimize losses. The number of modules required to build an SCA depends on the power required and also on the types of modules used and the operating conditions (solar radiation, temperature, etc.).

4.2 Basics for the Proposed Method

In Figure 12 the SCA characteristics for two different configurations ($N_p \times N_s = 2 \times 3$ and 1×6 with N_s : modules number in series and N_p branches number in parallel)

as well as that of two different loads Z_a and Z_b are plotted. In this case, the irradiance and temperature are kept constant. As can be seen the power corresponding to point A_1 is higher than that of point A_2 , which means that the first configuration (2x3) provides better load matching for this load than the second configuration (1x6). Whereas for load Z_b , the power on point B_1 is higher than that of point B_2 , which means that in this case the second configuration is better. It is then necessary to select on line and in real time the SCA appropriate configuration for a given load and under given working conditions in order to reduce the mismatch losses [3] [13-14].

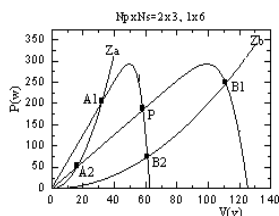


Figure 12
The P-V SCA and loads characteristics

Figure 12 shows that the two P-V SCA characteristics intersect on a point noted 'P'. At this operating point, either configuration could be used. Point 'P' is taken as a reference. For loads where their operating points are at the point 'P' left, configuration 1 (noted series configuration) should be used. And for all loads with operating points situated at the point 'P' right, configuration 2 (noted parallel configuration) is to be used. Therefore it is necessary to find a way to determine on line the point's 'P' position: the voltage V_{com} and the current I_{com} corresponding to this point. Then, the load voltage and current is compared to V_{com} and I_{com} . The SCA switches then onto the appropriate configuration.

4.3 Our Adopted Method

The principle of the proposed method consists of determining On-Line and in Real-Time for a fixed number of photovoltaic modules which configuration is the best for a given load under given working conditions and the switching the SCA into that configuration. Unfortunately, the reference point P is not fixed but varies with weather conditions (solar radiation, temperature, etc.). Therefore, it is necessary to determine the positions of point P as these conditions change; in other words, to find a way to determine the current (I_{com}) and the voltage (V_{com}) corresponding to point P as these conditions vary. A simulation program has been written to determine the variation of the commutation point as the solar radiation and/or the temperature change. Figures 13 and 14 show the simulation results for an SCA made of 6 modules, allowed to commute between two configurations (1X6 and 3X2) [3].

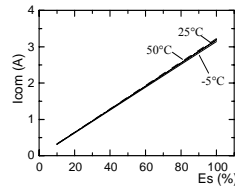


Figure 13

Variation of I_{com} versus solar radiation and temperatures

From Figure 13, it is clear that the commutation current varies linearly with the solar radiation and is hardly affected by the temperature. The simulation program has been run for other different configurations and the results led to the same conclusion. Consequently the current I_{com} could be written as follows.

$$I_{com} = K_i \cdot E_s \quad (19)$$

where E_s is the solar radiation and K_i is a constant which depends on the number and the type of modules used.

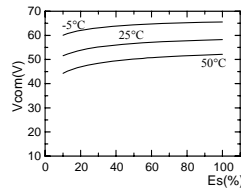


Figure 14

Variation of V_{com} versus solar radiation and temperatures

The variation of V_{com} as a function of the solar radiation for different temperatures has been determined and is illustrated in Figure 15. As can be seen, the characteristic is non linear at a low solar radiation level, so a simple linear procedure has been applied. As a consequence, for a given temperature the commutation voltage V_{com} could be written as follows:

$$V_{com} = a_i \cdot E_s + b_i \quad (20)$$

where a_i and b_i are constants which are derived from the linear procedure at 25°C. The Figure also shows that the commutation voltage V_{com} is significantly affected by the temperature T . As T increases V_{com} diminishes linearly. To implement the reconfiguration method using the commutation voltage V_{com} as reference, equation (20) should be corrected in order to take into account the linear variation of V_{com} as a function of the temperature.

After modification equation (20) becomes

$$V_{com} = a_i \cdot E_s + b_i + A_i \cdot (T - 25) \quad (21)$$

where a_i and b_i are as defined previously and A_i is the slope of the curve $V_{com} = f(T)$ at 25°C.

4.4 Practical Results

The control system based on equations (19) and (21) has been implemented (Figure 15) and an example of the practical results is given in Figure 16 [3].

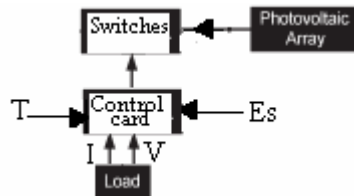


Figure 15

Our experimental system realized

A variable load has been used in order to cover different operating conditions. As can be seen, the SCA is switched into the appropriate configuration (Figure 16).

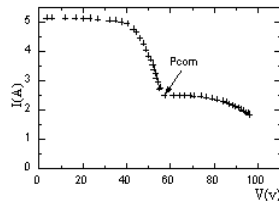


Figure 16

Practical characteristic I-V of the GP using the reconfiguration method at $E_s=78\%$, $T=27^\circ\text{C}$

Conclusion

The purpose of the work is to optimize the system's operation. The main reason for the described methods is to supply in an efficient manner a stand alone system using renewable energy sources such as photovoltaic ones. This study presents a simple but efficient method to improve a photovoltaic system's operation. The aim of the first method is to reach the MPP rapidly, in real time and automatically. It is used to maximize the photovoltaic array output power, irrespective of the temperature and irradiation conditions and of the load electrical characteristics. Thus, a new concept to track the MPP rapidly has been developed. The second method is an optimum switching of photovoltaic (PV) connected to a load, in real time. By rearranging the series and parallel connections between different modules, the matching between the load and SCA is improved. This enables the system to react to changes in loads and environmental conditions such as temperature and irradiance. The quality of load matching in a PV power system is improved by these proposed methods because the power available to the load is greater, whatever the changes in the load and/or in the climatic conditions. The experimental results show that the use of the two proposed method's control increases the PV output power. Our methods are in real time. Then, these methods take physical variations and aging of SCA and other effects such as shading into account.

References

- [1] Tiberiu Tudorache, Mihail Popescu: FEM Optimal Design of Wind Energy-based Heater, *Acta Polytechnica Hungarica*, Vol. 6, No. 2, 2009, pp. 55-70
- [2] Appelbaum J: The Operation of Loads Powered by Separate Sources or by a Common Source of Solar Cells: *IEEE Transactions on Energy Conversion*; Vol. 4, No. 3, September 1989, pp. 351-357
- [3] Zerhouni F. Z: Développement et optimisation d'un générateur énergétique hybride propre à base de PV-PAC, Doctoral thesis, university of sciences and technology Mohamed Boudiaf USTOMB, Algeria, 2009
- [4] V. Salas, E. Olias, A. Barrado, A. Lazaro: Review of the Maximum Power Point Tracking Algorithms for Stand Alone Photovoltaic Systems, *Solar Energy Materials & Solar Cells*, Vol. 90, 2006, pp. 1555-1578
- [5] Daiki Tokushima, Masato Uchida, Satoshi Kanbei, Hiroki Ishikawa, Haruo Naitoh: A New MPPT Control for Photovoltaic Panels by Instantaneous Maximum Power Point Tracking, *Electrical Engineering in Japan*, Vol. 157, No. 3, November 2006, pp. 73-800
- [6] Chen-Chi Chu, Chieh-Li Chen: Robust Maximum Power Point Tracking Method for Photovoltaic Cells: A Sliding Mode Control Approach, *Solar Energy*, Vol. 83, 2009, pp. 1370-1378
- [7] D. Brunelli, D. Dondi, A. Bertacchini, L. Larcher, P. Pavan, L. Benin: Photovoltaic Scavenging Systems: Modeling and Optimization *Microelectronics Journal*, 2009, pp. 1337-1344
- [8] Weidong Xiao, Student Member, Magnus G. J. Lind, William G. Dunford, and Antoine Capel: Real-Time Identification of Optimal Operating Points in Photovoltaic Power Systems, *IEEE Transactions on Industrial Electronics*, Vol. 53, No. 4, August 2006, pp. 1017-1026
- [9] Enrique M. a, E. Dura'n a, Sidrach-de-Cardona bM., Andu' jar J. M: Theoretical Assessment of the Maximum Power Point Tracking Efficiency of Photovoltaic Facilities with Different Converter Topologies, *Solar Energy*, Vol. 81, 2007, pp. 31-38
- [10] Liu Liqun, Wang Zhixin: A Variable Voltage MPPT Control Method for Photovoltaic Generation System, *wseas transactions on circuits and systems*, Vol. 8, No. 4, April 2009, pp. 335-349
- [11] Arias, J, Linera, F. F, Martin-Ramos, J, Pernia, A. M, Cambronero, J: A Modular PV Regulator Based on Microcontroller with Maximum Power Point Tracking, *Industry Applications*, 39th IAS Annual Meeting, conference Record of IEEE, 2, 2004, pp. 1178-1184, Industry Application Society Annual Meeting IAS'2004, Seattle,USA
- [12] Weidong Xiao, Nathan Ozog, William G. Dunford: Topology Study of Photovoltaic Interface for Maximum Power Point Tracking, *IEEE*

Transactions on Industrial Electronics, Vol. 54, No. 3, June 2007, pp. 1696-1704

- [13] Salameh, Z. M., Liang, C: Optimum Switching Points for Array Reconfiguration Controller, Conference Record of the Twenty First IEEE, Vol. 2, 1990, pp. 971-976
- [14] Salameh Z. M, Mulpur A. K., Dagher F: Two Stage Electrical Array Reconfiguration Controller, Solar Energy, Vol. 44, 1990, pp. 51-55